

# Hydrogen Peroxide Production in the Oxygen Reduction Reaction at Different Electrocatalysts as Quantified by Scanning Electrochemical Microscopy

Carlos M. Sánchez-Sánchez and Allen J. Bard\*

Center for Electrochemistry and the Department of Chemistry and Biochemistry, The University of Texas at Austin, Austin, Texas 78712

We present data for H<sub>2</sub>O<sub>2</sub> production at eight different materials tested as electrocatalysts for the oxygen reduction reaction (ORR) in 0.5 M H<sub>2</sub>SO<sub>4</sub> (Hg, Au, Ag, Cu, Pt, Pd, Pd<sub>80</sub>Co<sub>20</sub>, and Au<sub>60</sub>Cu<sub>40</sub>) using scanning electrochemical microscopy (SECM) as an alternative to the widely used rotating ring-disk electrode (RRDE) method. The amount of H<sub>2</sub>O<sub>2</sub> is related to the total number of electrons, *n*, found in the O<sub>2</sub> reduction reaction, with *n* = 2 showing only H<sub>2</sub>O<sub>2</sub> production and *n* = 4 showing no H<sub>2</sub>O<sub>2</sub> formation. From the SECM study Hg shows *n* close to 2, whereas Pt and Pd<sub>80</sub>Co<sub>20</sub> show *n*-values near 4. The other materials show intermediate *n*-values as a function of potential.

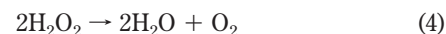
The discovery of inexpensive, stable, and highly efficient electrocatalysts for the oxygen reduction reaction (ORR) represents a major challenge in the development of polymer electrolyte membrane fuel cells (PEMFC) as a useful energy source.<sup>1,2</sup> The search for such materials useful at low temperatures in aqueous media has been widely carried out.<sup>3–5</sup> H<sub>2</sub>O<sub>2</sub> formation during the ORR is generally undesirable, as it lowers the efficiency and can lead to electrocatalyst corrosion and the chemical degradation of the membrane in the PEMFC.<sup>6</sup> In the PEMFC, the desired overall reaction involves 4e to produce only H<sub>2</sub>O, reaction 1.



This represents the overall thermodynamically favored path, but this cannot occur as one elementary step mechanistically because of the complexity of the reaction, involving 4e, 4 protons, and an

O–O bond cleavage. H<sub>2</sub>O<sub>2</sub> can be generated during the ORR as the final product or as an intermediate depending on the electrocatalytic material where the reaction takes place. The ORR reaction in acidic solution is complex and a number of mechanisms have been proposed for the reduction of O<sub>2</sub> to H<sub>2</sub>O<sub>2</sub> and H<sub>2</sub>O.<sup>7</sup> The two most favored are the peroxide and the metal oxide routes.

The peroxide pathway involves the initial production of superoxide ion (O<sub>2</sub><sup>•-</sup>), followed by additional protonation and electron transfer steps to produce H<sub>2</sub>O<sub>2</sub>. This is followed by additional steps, like H<sub>2</sub>O<sub>2</sub> disproportionation or reduction, to lead to H<sub>2</sub>O. For the purpose of this paper, overall reactions of interest in this general route are



The metal oxide route involves initial reaction of O<sub>2</sub> with a metal (as in corrosion reactions) followed by the reduction of the resultant metal oxide:



These reactions can occur in series or in parallel and lead to different overall amounts of H<sub>2</sub>O<sub>2</sub> produced and number of electrons transferred (*n*). Although reaction 1 is not known to occur mechanistically, a combination of the other reaction paths, e.g., reactions 2 + 3, 2 + 4, and 5 + 6 are equivalent to the overall 4-electron pathway of reaction 1.

Discerning among the different possible mechanisms for the ORR at different electrodes is very difficult. Methods such as rotating disk electrode (RDE) voltammetry have been used to study the current–potential curve and determine the overall *n*-value during the ORR, but these methods provide only an average value of *n* over the potential window studied. Moreover, it is very dangerous to try to discover a mechanism based solely

(7) Yeager, E. *Electrochim. Acta* 1984, 29, 1527.

\* To whom correspondence should be addressed. E-mail: ajbard@mail.utexas.edu.

- (1) Adzic, R. R. In *Electrocatalysis*; Lipkowsky, J., Ross, P. N., Eds.; Wiley-VCH: New York, 1998; Chapter 5.
- (2) O'Hayre R.; Suk-Won, C.; Colella, W.; Prinz, F. B. *Fuel Cell Fundamentals*; Wiley, New York, 2006.
- (3) Stamenkovic, V. R.; Mun, B. S.; Arenz, M.; Mayrhofer, K. J. J.; Lucas, C. A.; Wang, G.; Ross, P. N.; Markovic, N. M. *Nat. Mater.* 2007, 6, 241.
- (4) Bashyam, R.; Zelenay, P. *Nature* 2006, 443, 63.
- (5) Wang, B. J. *Power Source* 2005, 152, 1.
- (6) Borup, R.; Meyers, J.; Pivovar, B.; Kim, Y. S.; Mukundan, R.; Garland, N.; Myers, D.; Wilson, M.; Garzon, F.; Wood, D.; Zelenay, P.; More, K.; Stroh, K.; Zawodzinski, T.; Boncella, J.; McGrath, J. E.; Inaba, M.; Miyatake, K.; Hori, M.; Ota, K.; Ogumi, Z.; Miyata, S.; Nishikata, A.; Siroma, Z.; Uchimoto, Y.; Yasuda, K.; Kimijima, K.; Iwashita, N. *Chem. Rev.* 2007, 107, 3904.

on a single parameter, like  $n$  or the transmission coefficient,  $\alpha$ , as is sometimes done. The rotating ring-disk electrode (RRDE) technique provides additional information during the ORR at the disk as a function of the applied electrode potential by the quantification of the  $\text{H}_2\text{O}_2$  generated by oxidation at the ring. Such measurements can help gauge the relative importance of the peroxide routes in the overall ORR. However a large variety of  $n$  values can be found in the literature for identical materials, probably because the history of the electrocatalytic material under study can significantly affect the reaction rates; for example, in addition to the oxidation of  $\text{H}_2\text{O}_2$  at the ring which produces an anodic current, decomposition of the  $\text{H}_2\text{O}_2$  without current flow, i.e., reaction 4, can occur. In addition the potential of the platinum ring used as a detector in the RRDE can influence the  $n$ -value, e.g., by changing the relative amounts of platinum oxide formed, and differences in the synthesis conditions of the studied electrocatalysts can play a role. In this work we address the  $n$ -value quantification using the substrate generation-tip collection (SG/TC) mode of scanning electrochemical microscopy (SECM) to quantify the  $\text{H}_2\text{O}_2$  production at eight different electrode materials in acidic media. This method of  $\text{H}_2\text{O}_2$  quantification involves only diffusion, not convection, as with the RRDE, and yields higher collection efficiency values improving the precision of the measurement in comparison to the RRDE. In the RRDE, the collection efficiency depends on the ring and disk radii and the spacing between them and typically do not yield collection efficiencies higher than 20–30%. As we show in this study, we can readily obtain tip collection efficiencies of 43–49%. Moreover with SECM the sample is a small spot on the substrate, while with the RRDE, the sample must be used as the disk material, which often presents a significant fabrication cost.

SECM has found use in an increasing number of applications for the study of different electrocatalytic processes, such as hydrogen oxidation,<sup>8,9</sup> oxygen reduction,<sup>10,11</sup> methanol interference during ORR,<sup>12</sup> and oxygen evolution.<sup>13</sup> In particular, the SG/TC mode of the SECM has been of interest as a means of quantifying  $\text{H}_2\text{O}_2$  production during the ORR; two different SECM approaches have been used. In a previous paper<sup>14</sup> we presented the calibration equations based on simulations for carrying out the  $\text{H}_2\text{O}_2$  quantification under steady state conditions at small electrodes. This method utilized a steady-state SG/TC approach, where the substrate material was an ultramicroelectrode carrying out the ORR (equivalent to the disk in an RRDE experiment) and the tip detected  $\text{H}_2\text{O}_2$  by its oxidation (equivalent to the ring of the RRDE). This approach was validated for a Hg electrode, which produces  $\text{H}_2\text{O}_2$  as the

sole final product, reaction 2. A recent paper from the Wittstock group<sup>15</sup> shows another useful approach, where a transient SG/TC mode of SECM was used to detect  $\text{H}_2\text{O}_2$  during the ORR at macroscopic electrodes. This approach is based on the calculation of effective rate constants for the different reaction paths involved in the ORR and the determination of concentration profiles of  $\text{H}_2\text{O}_2$ . We present here  $\text{H}_2\text{O}_2$  quantification based on our SG/TC approach during the ORR in acidic solution for eight different electrocatalysts.

## EXPERIMENTAL SECTION

**Chemicals.** Copper wire (Puratronic, 99.9999%), silver wire (Premion, 99.997%), palladium wire (Premion, 99.99%),  $\text{HAuCl}_4 \cdot 3\text{H}_2\text{O}$ ,  $\text{Cu}(\text{NO}_3)_2 \cdot 3\text{H}_2\text{O}$ ,  $(\text{NH}_4)_2\text{PdCl}_4$ ,  $\text{Co}(\text{NO}_3)_2 \cdot 6\text{H}_2\text{O}$ , glycerol, glassy carbon (GC) plates, 1 mm thick (all Alfa Aesar, Ward Hill, MA), platinum wire (99.99%), and gold wire (99.99%) (Aldrich, St. Louis, MO),  $\text{H}_2\text{SO}_4$ , 94–98% trace metal grade (Fisher, Canada),  $\text{HNO}_3$  50–70%,  $\text{KNO}_3$  (Fisher, Fair Lawn, NJ), and  $\text{Hg}_2(\text{NO}_3)_2$  dihydrate (Fluka, Steinheim, Germany) were used as received. Deionized water was obtained from a Milli-Q (Millipore) system.

**Electrodes.** The usual parameters to define a SECM tip are  $a$  (tip radius),  $r_g$  (tip radius including the glass sheath) and RG value ( $\text{RG} = r_g/a$ ). In the SG/TC experiments, the size of the substrate is also important and should be relatively small to yield a high tip collection, so 100  $\mu\text{m}$  diameter Au, Ag, Cu, Pt, and Pd electrodes with  $\text{RG} = 17$ – $20$  and 25  $\mu\text{m}$  diameter Pt and Au ultramicroelectrodes (UME) with  $\text{RG} = 6$ – $12$  were fabricated by heat sealing the corresponding metal wire under vacuum in a borosilicate glass capillary.<sup>16</sup> A 100  $\mu\text{m}$  diameter Hg electrode was prepared by Hg electrodeposition on a 100  $\mu\text{m}$  diameter Au electrode following the procedure described in the literature.<sup>17</sup> All these substrate and tip electrodes were polished with alumina paste (0.05  $\mu\text{m}$ ) on microcloth pads (Buehler, Lake Bluff, IL) to yield a flat disk. Following the procedure previously described<sup>10</sup> for synthesizing metallic spots supported on GC using a picoliter solution dispenser, three different samples were prepared: (i) a high-density Au–Cu array formed by spots of different Au–Cu composition, (ii) a single catalyst spot of  $\text{Pd}_{80}\text{Co}_{20}$  (100  $\mu\text{m}$  diameter), and (iii) a single catalyst spot of  $\text{Au}_{60}\text{Cu}_{40}$  (200  $\mu\text{m}$  diameter). All three samples were prepared dispensing on the GC support solutions containing 0.3 M metal ion prepared by dissolving the corresponding metal precursor salt ( $\text{HAuCl}_4 \cdot 3\text{H}_2\text{O}$ ,  $\text{Cu}(\text{NO}_3)_2 \cdot 3\text{H}_2\text{O}$ ,  $(\text{NH}_4)_2\text{PdCl}_4$  and  $\text{Co}(\text{NO}_3)_2 \cdot 6\text{H}_2\text{O}$ ) in water-glycerol (3:1) and using the pL-solution dispenser (CHI 1550, Austin TX). The spots were dried under Ar at 150  $^\circ\text{C}$  overnight and then reduced under  $\text{H}_2$  at 350  $^\circ\text{C}$  for 1 h in a tube furnace. A homemade reversible hydrogen electrode (RHE) was used as the reference in all experiments. It was assembled before each experiment following our previously described procedure.<sup>12</sup> The potential of our RHE was stable during the entire experimental time period. All potentials in the text are reported with respect to a RHE. A gold wire or a graphite rod, 0.5 mm diameter, was used as a counter electrode. Note that it is

(8) Shah, B. C.; Hillier, A. C. *J. Electrochem. Soc.* **2000**, *147*, 3043.

(9) Jayaraman, S.; Hillier, A. C. *Langmuir* **2001**, *17*, 7857.

(10) Fernandez, J. L.; Walsh, D. A.; Bard, A. J. *J. Am. Chem. Soc.* **2005**, *127*, 357.

(11) Walsh, D. A.; Fernandez, J. L.; Bard, A. J. *J. Electrochem. Soc.* **2006**, *153*, E99.

(12) Lin, C. L.; Sanchez-Sanchez, C. M.; Bard, A. J. *Electrochem. Solid-State Lett.* **2008**, *11*, B136.

(13) Minguzzi, A.; Alpuche-Aviles, M. A.; Rodriguez-Lopez, J.; Rondinini, S.; Bard, A. J. *Anal. Chem.* **2008**, *80*, 4055.

(14) Sanchez-Sanchez, C. M.; Rodriguez-Lopez, J.; Bard, A. J. *Anal. Chem.* **2008**, *80*, 3254.

(15) Shen, Y.; Trauble, M.; Wittstock, G. *Anal. Chem.* **2008**, *80*, 750.

(16) *Scanning Electrochemical Microscopy*; Bard, A. J., Mirkin, M. V., Eds.; Marcel Dekker: New York, 2001.

(17) Selzer, Y.; Turyan, I.; Mandler, D. *J. Phys. Chem. B* **1999**, *103*, 1509.

important to use a counter electrode that cannot deposit an active metal on the substrate during the experiment; Pt counter electrodes were never used.

**Electrochemical Measurements.** All electrochemical measurements were carried out at room temperature in a four-electrode arrangement using the CHI 900B SECM (CH Instruments, Austin, TX), which incorporates a bipotentiostat.

(a) *H<sub>2</sub>O<sub>2</sub> Quantification during ORR Using the SG/TC Mode of the SECM.* Following the procedure described in our previous paper,<sup>14</sup> the SG/TC experiment for H<sub>2</sub>O<sub>2</sub> quantification during ORR was carried out for all eight different electrocatalysts studied in an oxygen saturated 0.5 M H<sub>2</sub>SO<sub>4</sub> solution. Briefly, the Pt UME, used as the collector tip, was located at a given tip-substrate distance above the center of the substrate electrode in an O<sub>2</sub> saturated 0.5 M H<sub>2</sub>SO<sub>4</sub> solution. Then, a linear scan voltammogram (LSV) of the substrate was taken while the tip potential was held at a constant value of 1.2 V where the H<sub>2</sub>O<sub>2</sub> generated at the substrate is oxidized under diffusion controlled conditions. A low scan rate, 2 mV/s, was used during the substrate potential sweep to allow steady-state concentrations to be achieved. The substrate electrode was tightened at the bottom of a Teflon cell with either a 2.0 mm (for substrates constructed as tips) or 6.5 mm (for spots supported on GC) diameter aperture via an O-ring. The tip radius (*a*) and RG, the substrate radius (*b*), and the tip-substrate distance (*d*) are the important parameters in this SG/TC experiment to determine the maximum collection efficiency (CE<sup>max</sup>) achievable according to the calibration equations reported in our previous paper.<sup>14</sup> Before processing the tip and substrate currents obtained from the SG/TC experiment and calculating the *n*-value for ORR at the studied electrocatalyst using eq 7, the tip current was normalized by subtracting the corresponding background current. When the studied electrocatalyst was supported on a GC plate, it was necessary to subtract the background contribution in an oxygen-free solution from the total substrate current recorded.

$$n = \frac{4i_{\text{subs}}}{\left[ i_{\text{subs}} + \left| \frac{i_{\text{tip}}}{\text{CE}^{\text{max}}/100} \right| \right]} \quad (7)$$

(b) *SECM SG/TC Imaging of a Single Electrocatalyst.* A SG/TC image of a single material was obtained using the same setup that we used to quantify H<sub>2</sub>O<sub>2</sub> during the ORR. A 25 μm diameter Pt UME tip was located at a constant tip-substrate distance (*d* = 40–50 μm) and its potential was held constant at 1.2 V, where the H<sub>2</sub>O<sub>2</sub> generated at the substrate is oxidized under diffusion controlled conditions. Then, the substrate potential was held at a constant potential in an active region for ORR and the H<sub>2</sub>O<sub>2</sub> oxidation current detected at the tip was recorded as a function of tip position. The tip was scanned in the X–Y plane above a single electrocatalyst spot supported on either GC (Pd<sub>80</sub>Co<sub>20</sub>) or surrounded by glass (Cu) in an oxygen saturated 0.5 M H<sub>2</sub>SO<sub>4</sub> solution.

(c) *SECM Tip Generation-Substrate Collection (TG/SC) Imaging of an Array.* Following the procedure previously reported,<sup>10</sup> a constant O<sub>2</sub> flow was generated at a 25 μm diameter Au UME tip using a 9 V battery connected between the tip and a gold auxiliary electrode with a resistor limiting the O<sub>2</sub> generation

current at the tip. Then, this tip was located at a constant tip-substrate distance (*d* = 40 μm) keeping the tilt of the substrate at Δ*z*/Δ*x* (or Δ*y*) ≤ 1.5 μm/mm. The substrate potential was held constant in an active region for the ORR in an oxygen free solution. Then, the oxygen reduction current produced at the substrate when the oxygen generator tip was scanned in the X–Y plane above the Au–Cu array of spots on GC was recorded as a function of tip position. An argon blanket was maintained over the 0.5 M H<sub>2</sub>SO<sub>4</sub> solution during the experiment to keep the solution free from atmospheric oxygen.

## RESULTS AND DISCUSSION

### SG/TC with Metals with Negligible H<sub>2</sub>O<sub>2</sub> Heterogeneous Decomposition Rate in Acidic Media: Hg, Au, Ag, and Cu.

In this case the peroxide generation is followed by little H<sub>2</sub>O<sub>2</sub> decomposition. Figure 1 shows the tip and substrate currents collected using the SG/TC mode of SECM during the ORR at Hg, Au, and Ag electrodes. The anodic tip current when Hg is the substrate (Figure 1A, red plot, right axis) reaches a stable maximum (–10.3 nA) for substrate potentials more negative than –0.15 V, which corresponds to the maximum O<sub>2</sub> reduction current reached at the substrate (Figure 1A, black plot, left axis). This indicates that the H<sub>2</sub>O<sub>2</sub> produced during the ORR on Hg is stable and does not undergo further reduction within the studied potential window. In contrast, Figure 1B (Au) and C (Ag) show a different tip current response within the corresponding potential window. When the ORR was carried out on Au, two different potential regions can be distinguished: 0.5 ≥ *E* > 0.15 V, where the tip current linearly increases up to –9.1 nA and H<sub>2</sub>O<sub>2</sub> is a stable final product and *E* ≤ 0.15 V, where the amount of H<sub>2</sub>O<sub>2</sub> detected decreases, while the O<sub>2</sub> reduction current continues to grow slightly, which is due to a larger number of electrons involved in the ORR. The drop in the H<sub>2</sub>O<sub>2</sub> detected is more evident with a Ag substrate (Figure 1C), since a sharp decrease in the H<sub>2</sub>O<sub>2</sub> collected is observed at potentials more negative than 0.025 V (from *I*<sub>tip</sub> = –4.9 nA to –1.1 nA). We assign this drop in the H<sub>2</sub>O<sub>2</sub> detected during ORR on Au and Ag after certain potential to the occurrence of a second reaction, H<sub>2</sub>O<sub>2</sub> reduction. Results showing a clear transition from two electrons during ORR at low overpotentials to four electrons at high overpotentials has been recently reported at Ag(111) single crystal in HClO<sub>4</sub> 0.1 M solution.<sup>18</sup>

Cu undergoes corrosion in an oxygenated 0.5 M H<sub>2</sub>SO<sub>4</sub> solution at its open circuit potential, which involves O<sub>2</sub> reduction to form mainly H<sub>2</sub>O<sub>2</sub> with simultaneous Cu oxidation. This is shown in Figure 2, where the tip current, which represents H<sub>2</sub>O<sub>2</sub> collection, increases to 10 times that of the background when the tip scans above the Cu substrate held at open circuit (the Cu substrate is marked with a black circle in the SECM image). Because of this corrosion reaction, for the Cu case, all scans were taken from the negative potential limit toward the positive in order to start with a negligible oxidation current at the tip (note that all scans for the other materials were always carried out from positive potentials toward more negative ones). Figure 3 shows the tip and substrate currents collected using the SG/TC mode of SECM during the ORR at Cu electrode. The

(18) Bliznac, B. B.; Ross, P. N.; Markovic, N. M. *Electrochim. Acta* **2007**, *52*, 2264.



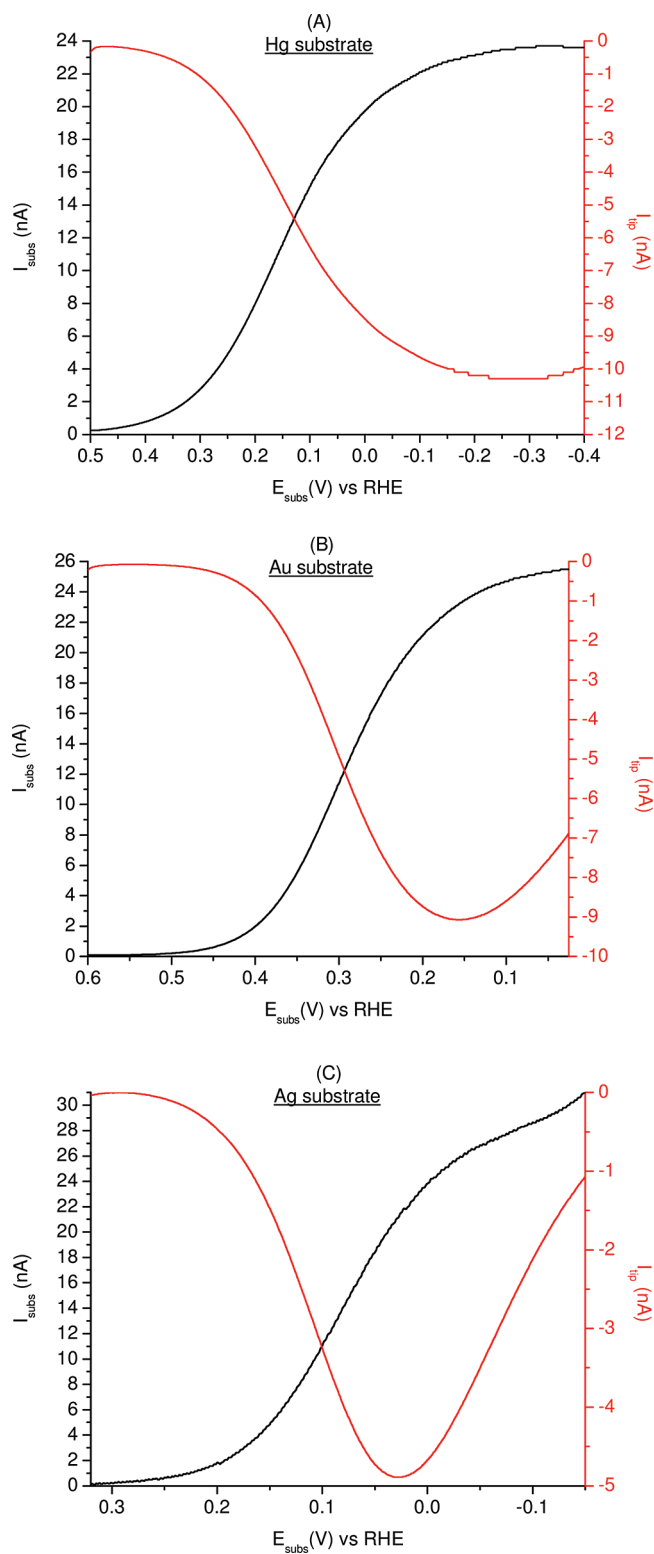


**Figure 1.** ORR in an oxygen saturated 0.5 M  $\text{H}_2\text{SO}_4$  solution at 100  $\mu\text{m}$  diameter Hg, Au, and Ag substrates (black lines) and simultaneous  $\text{H}_2\text{O}_2$  quantification at a Pt tip (25  $\mu\text{m}$  diameter) (red lines) using the SG/TC mode of SECM. Tip RG = 6 and  $d = 10 \mu\text{m}$  ( $\text{CE}^{\text{max}} = 49\%$ ). (A) Hg; (B) Au; (C) Ag.

tip current at Figure 3 (red line) is negligible for substrate potentials less positive than 0.125 V, although appreciable cathodic substrate current flows. The tip current increases sharply at more positive potentials, with  $\text{H}_2\text{O}_2$  quantification on Cu limited by the Cu corrosion potential in this medium ( $\sim 0.24$  V). The high

$\text{H}_2\text{O}_2$  production near the Cu corrosion potential suggests  $\text{H}_2\text{O}_2$  production only at or near where corrosion of Cu occurs. The reduction at substrate potentials more negative than 0.125 V takes place without  $\text{H}_2\text{O}_2$  production. These results agree with several studies of the ORR on Cu single crystals using the RRDE in sulphuric acid solutions,<sup>19,20</sup> where the ORR was reported as a 2e or a 4e reaction, depending on  $\text{HSO}_4^-$  and  $\text{SO}_4^{2-}$  adsorption in the different potential regions.

Direct comparison of all substrate currents displayed in Figures 1 and 3 is not possible because of the different effective areas of the studied metals. For this reason, it is necessary to correlate tip and substrate currents using eq 7 to obtain useful mechanistic information through the calculation of the  $n$  value. From the SG/TC experiment results displayed in Figures 1 and 3 it is possible to calculate the  $n$  value during ORR at Hg, Au, Ag, and Cu as a function of the applied potential substituting the corresponding tip and substrate currents in eq 7, as discussed earlier.<sup>14</sup> Figure 4 shows the  $n$  value as a function of the applied potential. For Cu and Ag, one sees a noticeable change from the 2e toward the 4e path as the potential becomes more negative. On Hg, within the entire potential window studied, and on Au in the low overpotential region, the  $n$  value remains close to 2 following almost exclusively the 2e path during ORR. But the Au electrode in the high overpotential region starts a moderate transition toward higher  $n$  values. In all of these cases where the ORR occurs at potentials quite negative of the reversible 4e ORR potential, reaction 1, the calculation of the  $n$  value is limited in the negative potential region because of the beginning of the hydrogen evolution reaction.

**SG/TC with Metals with a High  $\text{H}_2\text{O}_2$  Heterogeneous Decomposition Rate: Pt, Pd, and  $\text{Pd}_{80}\text{Co}_{20}$ .** Most of the potentially useful electrocatalysts for the ORR in fuel cell applications carry out the reaction predominantly by the 4e path at significantly more positive potentials than the former group. Most also show a high  $\text{H}_2\text{O}_2$  heterogeneous decomposition rate, which in aqueous solution is very strongly influenced by the pH of the solution and is generally more rapid in alkaline than in acidic media. Some materials like Au are only active in strongly alkaline media,<sup>21</sup> but Pt and Pd electrodes also show substantial activity in 0.5 M  $\text{H}_2\text{SO}_4$ .<sup>22</sup> Thus  $\text{H}_2\text{O}_2$  quantification for ORR at Pt, Pd and  $\text{Pd}_{80}\text{Co}_{20}$ , a promising Pd-based electrocatalyst for ORR in fuel cells,<sup>10–12</sup> is also reported here. Figure 5 shows the tip and substrate currents collected using the SG/TC mode of SECM during the ORR at Pt, Pd and  $\text{Pd}_{80}\text{Co}_{20}$  electrodes. These materials can be brought to a much more positive starting potential for substrate potential scans than in Hg, Au, Ag, and Cu, because they are less prone to oxidation in acidic media. Moreover, Pt and  $\text{Pd}_{80}\text{Co}_{20}$  exhibit hardly noticeable  $\text{H}_2\text{O}_2$  collection currents (see  $I_{\text{tip}}$  scales in Figure 5). The  $\text{H}_2\text{O}_2$  collection current (red plot) for Pt and Pd in Figure 5A and B, is much smaller for Pt at a similar substrate generation current (black plot) (note difference in scales on the right and left axes). This is consistent with previously reported rate constants for  $\text{H}_2\text{O}_2$  decomposition for Pt and Pd in acidic

(19) Brisard, G.; Bertrand, N.; Ross, P. N.; Markovic, N. M. *J. Electroanal. Chem.* **2000**, *480*, 219.

(20) Jiang, T.; Brisard, G. M. *Electrochim. Acta* **2007**, *52*, 4487.

(21) McKee, D. W. *J. Catal.* **1969**, *14*, 355.

(22) Bianchi, G.; Mazza, F.; Mussini, T. *Electrochim. Acta* **1962**, *7*, 457.

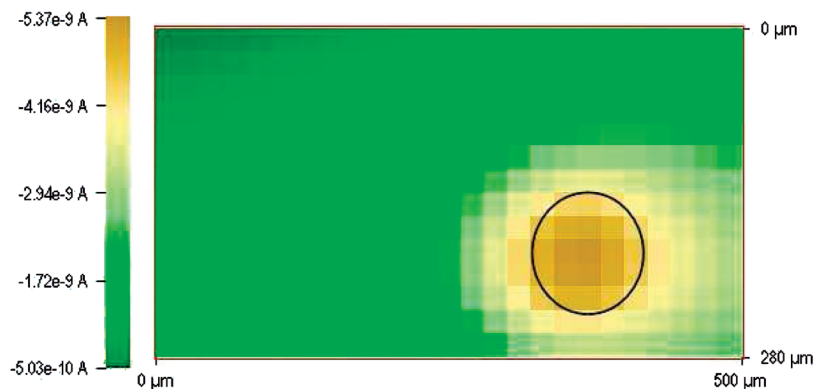


**Figure 2.** SECM SG/TC image displaying the tip current for  $\text{H}_2\text{O}_2$  collection scanning above a  $100\ \mu\text{m}$  diameter Cu substrate (circled area) embedded in glass. Tip–substrate distance =  $50\ \mu\text{m}$ . Tip potential =  $1.2\ \text{V}$  and Cu substrate at open circuit potential in an oxygen saturated  $0.5\ \text{M}\ \text{H}_2\text{SO}_4$  solution. Scan rate =  $100\ \mu\text{m}/\text{s}$ .

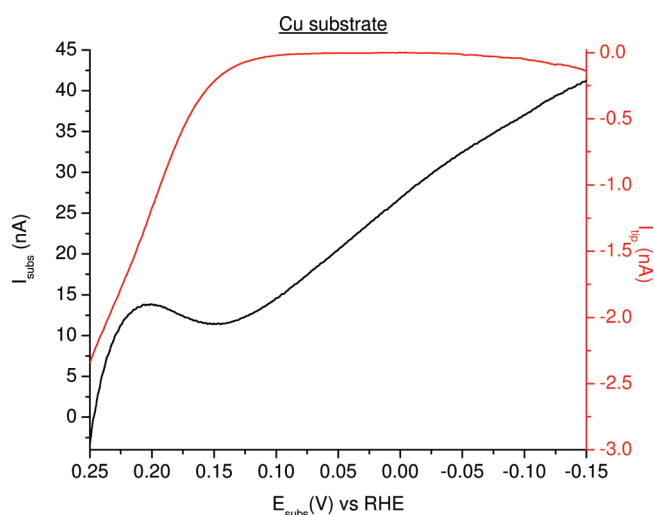


**Figure 3.** ORR at a Cu substrate ( $100\ \mu\text{m}$  diameter) in an oxygen saturated  $0.5\ \text{M}\ \text{H}_2\text{SO}_4$  solution (black line) and simultaneous  $\text{H}_2\text{O}_2$  quantification at a Pt tip ( $25\ \mu\text{m}$  diameter) (red line) using the SG/TC mode of SECM. Tip RG = 6 and  $d = 12\ \mu\text{m}$ . ( $\text{CE}^{\text{max}} = 44\%$ ).

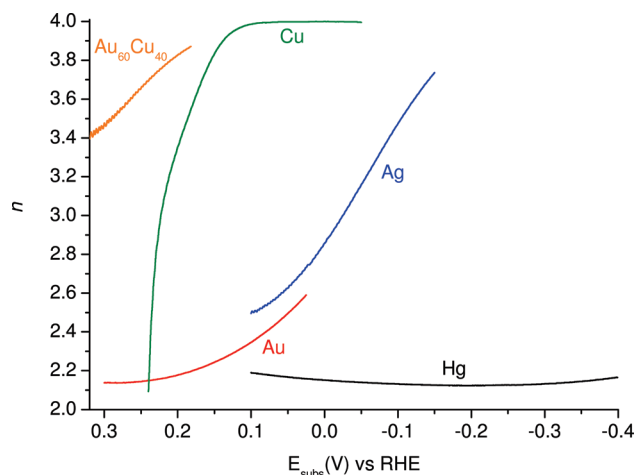


**Figure 4.** Number of electrons transferred ( $n$ ) during ORR at Hg (black line), Au (red line), Ag (blue line), Cu (green line), and  $\text{Au}_{60}\text{Cu}_{40}$  (orange line) as a function of applied potential in an oxygen saturated  $0.5\ \text{M}\ \text{H}_2\text{SO}_4$  solution.

$\text{Pd}_{80}\text{Co}_{20}$  spot supported on GC (Figure 5C) demonstrates that this technique is not limited to pure metals embedded in glass as substrates. The only difference in the study of electrocatalyst spots supported on GC is that it is necessary to subtract the contribution from the background; thus Figure 5C shows the net  $\text{O}_2$  reduction current (black plot) obtained after background subtraction. The present work demonstrates that not only does  $\text{Pd}_{80}\text{Co}_{20}$  shift the potentials for the ORR to more positive ones compared with pure Pd (see onset potentials at black plots in Figure 5B and C) as previously reported,<sup>10</sup> but  $\text{Pd}_{80}\text{Co}_{20}$  also greatly decreases  $\text{H}_2\text{O}_2$  generation as well (compare the  $\text{H}_2\text{O}_2$  collection current (red plot) for Pd and  $\text{Pd}_{80}\text{Co}_{20}$  in Figure 5B and C).

Figure 6 shows the  $n$  value variation as a function of the applied potential for Pt, Pd, and  $\text{Pd}_{80}\text{Co}_{20}$ . In all three cases, the calculation of the  $n$  value is limited by the start of hydrogen adsorption at the electrocatalyst in the less positive potential region. Among these three materials, Pt (black plot) shows an  $n$  value closest to the maximum, from  $n = 3.9$  to  $4.0$ . For Pd  $n$  varies from  $2.8$  to  $3.6$ , depending on potential. An  $n$  value of  $2.5$  for the ORR on Pd calculated from RDE measurements in  $0.5\ \text{M}\ \text{H}_2\text{SO}_4$  has been recently reported.<sup>23</sup> The  $\text{Pd}_{80}\text{Co}_{20}$  result (blue plot) is similar to that of Pt, with  $n$  values close to the maximum ( $n = 3.7$ – $4.0$ ). These large values agree with the average  $n$  value equal to  $4.0$  reported for ORR on  $\text{CoPd}_3$  nanoparticles calculated from RDE measurements in  $0.5\ \text{M}\ \text{H}_2\text{SO}_4$ .<sup>23</sup> The initial report of our research group<sup>10</sup> proposed that the improvement in the ORR activity of Pd by incorporation of Co exhibited in  $\text{Pd}_{80}\text{Co}_{20}$  could be based on the excellent properties of Co in splitting the oxygen bond, which mainly directs ORR through the metal oxide pathway, reactions 5 and 6. However, the results here show the production of a small amount of  $\text{H}_2\text{O}_2$  as well, so a small contribution of a peroxide pathway is suggested. Figure 7 shows a SECM image of  $\text{H}_2\text{O}_2$  collection current registered when the tip scans above a  $\text{Pd}_{80}\text{Co}_{20}$  spot held at  $0.4\ \text{V}$  (where  $n = 4.0$  according to Figure 6) and suggests that this material is also effective at catalyzing the disproportionation of  $\text{H}_2\text{O}_2$ , reaction 4. The current distribution in this Figure is different than the SG/TC image presented in Figure 2. The black circle in Figure 7 marks the substrate spot location and the collection current there is smaller than the collection current in the vicinity around the spot where  $\text{H}_2\text{O}_2$  can

solution, where the Pt rate constant is 19 times that for Pd.<sup>22</sup> The ability to study  $\text{H}_2\text{O}_2$  production during the ORR at a single

(23) Mustain, W. E.; Prakash, J. J. *Electrochem. Soc.* **2007**, *154*, A668.

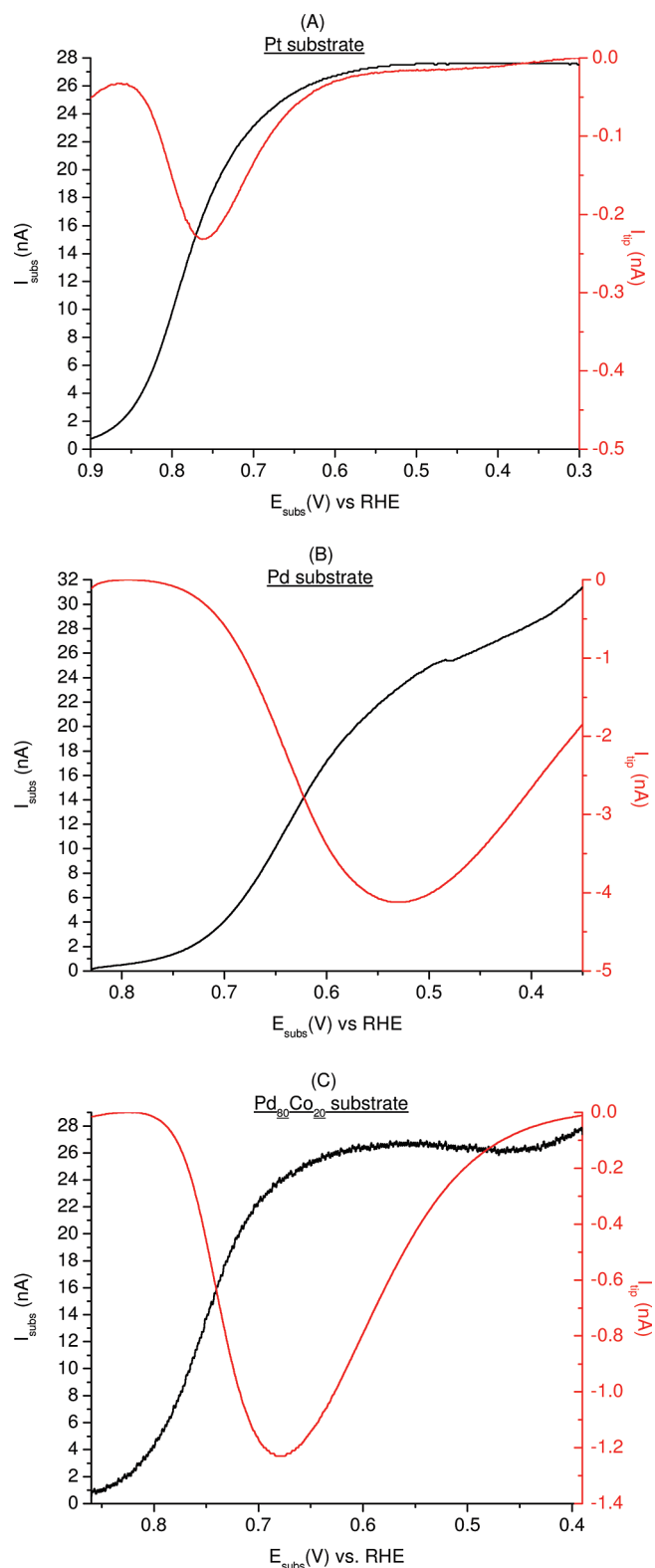


**Figure 5.** ORR in an oxygen saturated 0.5 M H<sub>2</sub>SO<sub>4</sub> solution at 100  $\mu$ m diameter Pt, Pd, and Pd<sub>80</sub>Co<sub>20</sub> spot substrates (black lines) and simultaneous H<sub>2</sub>O<sub>2</sub> quantification at a Pt tip (25  $\mu$ m diameter, RG = 6) (red lines) using the SG/TC mode of SECM,  $d = 10 \mu$ m (CE<sup>max</sup> = 49%) for Pt and Pd and  $d = 7 \mu$ m (CE<sup>max</sup> = 60%) for Pd<sub>80</sub>Co<sub>20</sub>. (A) Pt; (B) Pd; (C) Pd<sub>80</sub>Co<sub>20</sub>. Note the large difference in current scales for substrate (black) and tip (red).

diffuse away into the solution without undergoing any further reaction. Thus H<sub>2</sub>O<sub>2</sub> generated at the substrate perimeter can

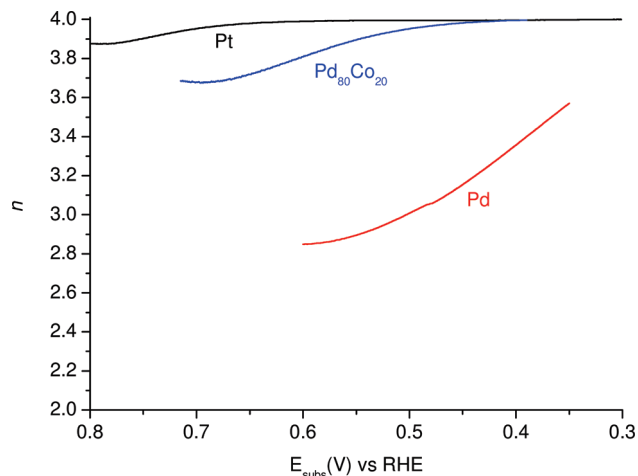


**Figure 6.** Number of electrons transferred ( $n$ ) during ORR at Pt (black line), Pd (red line) and Pd<sub>80</sub>Co<sub>20</sub> (blue line) as a function of applied potential in an oxygen saturated 0.5 M H<sub>2</sub>SO<sub>4</sub> solution.

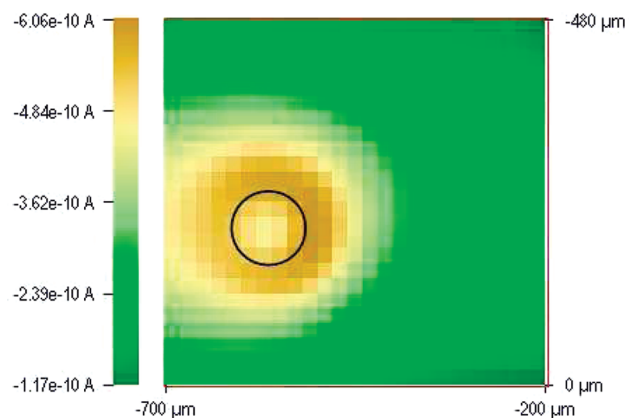


**Figure 7.** SECM SG/TC image displaying the tip current for H<sub>2</sub>O<sub>2</sub> collection above a single 100  $\mu$ m diameter Pd<sub>80</sub>Co<sub>20</sub> spot supported on GC (circled area). Tip-substrate distance = 40  $\mu$ m. Tip potential = 1.2 V and Pd<sub>80</sub>Co<sub>20</sub> substrate held at 0.4 V in an oxygen saturated 0.5 M H<sub>2</sub>SO<sub>4</sub> solution. Scan rate = 100  $\mu$ m/s.

diffuse away from the substrate surface and avoid the disproportionation step. This reaction step also can contribute to the overall activity of the catalyst for the ORR.

**The ORR at Au–Cu Mixtures.** To test the idea that H<sub>2</sub>O<sub>2</sub> decomposition, reaction 4, during the ORR can be related to the electrocatalyst activity, we investigated mixtures of Au–Cu. Au in acid media shows extensive generation of H<sub>2</sub>O<sub>2</sub> during the ORR, while Cu can achieve total reduction of oxygen to water ( $n = 4$ ) within most of the potential window where Cu does not undergo corrosion (see Figure 4). The TG/SC mode of the SECM has been successfully used for rapid imaging of arrays of bimetallic materials with different compositions for the ORR in 0.5 M H<sub>2</sub>SO<sub>4</sub> solution.<sup>10–12</sup> Following these well-established procedures for spot preparation and screening, we prepared an array composed by rows of spots with different atomic ratios of Au–Cu supported on a GC plate. The array was scanned in the X–Y plane in deaerated 0.5 M H<sub>2</sub>SO<sub>4</sub> with an Au UME tip held at a constant anodic current to generate a constant O<sub>2</sub> flow. The substrate reduction current at a given potential is a measure of the rate of the ORR when the tip is above a particular spot in the array. Figure 8 shows a SECM TG/SC image of the Au–Cu array (two replicate lines) with the substrate

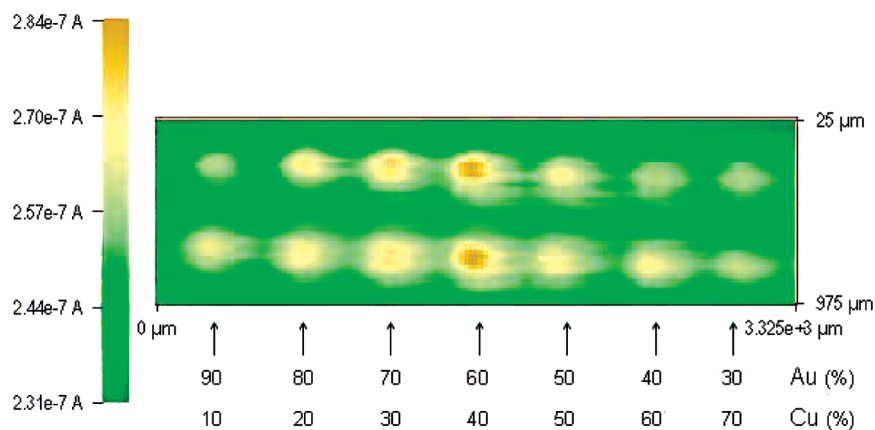


**Figure 8.** SECM TG/SC image displaying the substrate current for ORR of an array composed by two equal rows of spots with different atomic ratios of Au–Cu supported on GC. Tip-substrate distance = 40  $\mu\text{m}$ . Oxygen was generated at a constant current of  $-170$  nA at the tip. The substrate potential was held at 0.35 V in an oxygen-free 0.5 M  $\text{H}_2\text{SO}_4$  solution. Scan rate = 125  $\mu\text{m/s}$ .

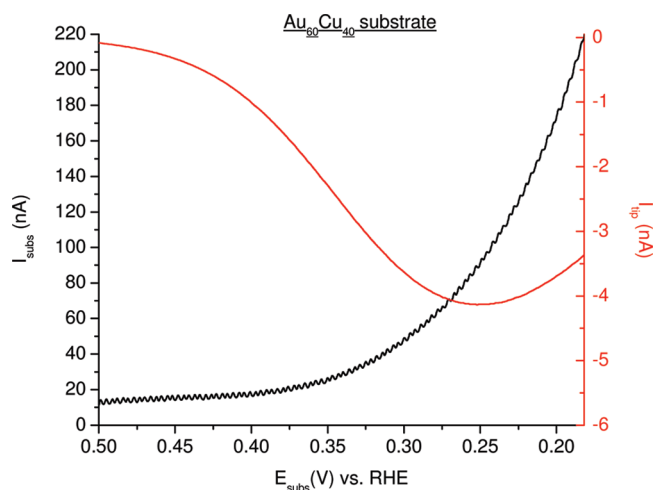


**Figure 9.** ORR at a  $\text{Au}_{60}\text{Cu}_{40}$  spot substrate (200  $\mu\text{m}$  diameter) supported on GC in an oxygen saturated 0.5 M  $\text{H}_2\text{SO}_4$  solution (black line) and simultaneous  $\text{H}_2\text{O}_2$  quantification at a Pt tip (25  $\mu\text{m}$  diameter) (red line) using the SG/TC mode of SECM. Tip RG = 12 and  $d = 10$   $\mu\text{m}$ . ( $\text{CE}^{\text{max}} = 43\%$ ).

potential at 0.35 V. The lower current value shown in the scale bar corresponds to the background current, which is mainly that of the GC and the metallic spots contributions and is a function of the total number of spots present in the sample. The results displayed in Figure 8 were obtained in triplicate at  $d = 40$   $\mu\text{m}$ . The TG/SC mode of SECM allows CE equal to 100%, but only for small  $d$  values. Thus, only the relative CE for the different spots can be directly obtained from the reduction currents displayed in this image. At 0.35 V, pure Cu is not stable with respect to corrosion and the pure Au spot cannot be distinguished from the background current because it exhibits low activity for the ORR. The spot composition corresponding to  $\text{Au}_{60}\text{Cu}_{40}$  showed the highest oxygen reduction activity in Figure 8. Although  $\text{Au}_{60}\text{Cu}_{40}$  is not a useful electrocatalyst for the ORR, because it does not exhibit oxygen reduction activity at potentials more positive than 0.6 V, the results demonstrate the synergistic effect of adding Cu to Au. Figure 9 shows the tip and substrate currents collected using the SG/TC mode of SECM described previously to quantify the amount of  $\text{H}_2\text{O}_2$  produced during the ORR at a large single  $\text{Au}_{60}\text{Cu}_{40}$  spot (200  $\mu\text{m}$  diameter) prepared in the same way as the array spots.

Figure 4 (orange plot) shows the  $n$  value variation ( $n = 3.4\text{--}3.9$ ), as a function of the applied potential for ORR at  $\text{Au}_{60}\text{Cu}_{40}$ . Clearly, incorporation of Cu into Au increases the overall  $n$  value compared to Au. One interpretation of this result is that Cu decreases the amount of  $\text{H}_2\text{O}_2$  produced. However, this result can also be interpreted in terms of the previously proposed metal oxide mechanism consistent with several previous bimetallic combinations.<sup>10,11</sup>

## CONCLUSIONS

Quantification of the  $\text{H}_2\text{O}_2$  generated at the electrocatalyst surface during the ORR is important in evaluating potential performance, e.g., in fuel cells and air batteries. The SG/TC mode of the SECM is a useful and powerful alternative to the RRDE for  $\text{H}_2\text{O}_2$  quantification.  $\text{H}_2\text{O}_2$  formation during the ORR with eight different materials (Hg, Au, Ag, Cu, Pt, Pd,  $\text{Pd}_{80}\text{Co}_{20}$ , and  $\text{Au}_{60}\text{Cu}_{40}$ ) in 0.5 M  $\text{H}_2\text{SO}_4$  solution was studied with the SECM. Hg is the only material that shows an  $n$  value that is very close to the minimum ( $n = 2$ ), for exclusive production of  $\text{H}_2\text{O}_2$  during ORR over the entire potential window. In contrast, Pt and  $\text{Pd}_{80}\text{Co}_{20}$  exhibit  $n$  values much closer to the maximum ( $n = 4$ ), denoting total  $\text{O}_2$  reduction to  $\text{H}_2\text{O}$  and also effective catalysis of the  $\text{H}_2\text{O}_2$  disproportionation reaction. Au, Ag, and Pd electrodes exhibit a gradual transition from lower to higher  $n$  values within the potential window studied. A Cu electrode shows a sharp transition from  $n = 2$ , at potentials close to the Cu corrosion potential, to  $n = 4$  at more negative values. We also screened Au–Cu mixtures with the SECM and identified  $\text{Au}_{60}\text{Cu}_{40}$  as the best Au–Cu composition for ORR. This material exhibited much lower  $\text{H}_2\text{O}_2$  production than Au alone during the ORR, but the potential region for oxygen reduction is significantly less positive than that needed for a good electrocatalyst.

## ACKNOWLEDGMENT

The National Science Foundation CHE-0451494 and CHE-0808927 and the Robert A. Welch Foundation (F-0021) and the Center for Electrochemistry have supported this work. C.M.S.-S. thanks the Ministerio Español de Educación y Ciencia and Fundacion Española para la Ciencia y la Tecnología for support of a postdoctoral fellowship.

Received for review June 15, 2009. Accepted August 6, 2009.

AC901291V